Theor Chim Acta (1989) 76: 137–145

Theoretica Chimica Acta

Quantum simulation of vibration states and Franck–Condon overlap in non-separable potentials

W. Lorenz and O. Heitzsch
Sektion Chemie, Karl-Marx-Universität Leipzig, DDR-7010 Leipzig, German Democratic Republic

(Received December 2, 1988; revised March 10/Accepted March 24, 1989)

Summary. Taking into consideration nuclear motion in non-separable potentials, we have probed the solution of the Schrödinger equation by random walk sampling in imaginary time on a two-dimensional example. Evaluation of the many-dimensional Franck-Condon overlap and the chemical species conversion rate is outlined.

Key words: Quantum simulation — Non-separable vibrations — Franck–Condon overlap

1. Introduction

Our aim in this paper is to prepare for further numerical exploration of local chemical processes in condensed systems or at interfaces [1, 2]. As a starting point of the following, we note that in the chemical species conversion probability expression

$$\langle P_{a\to b}\rangle = \frac{2\pi}{\hbar} Av|T_{ba}|^2\delta(\Delta E^{\text{vib}} + \Delta E), \tag{1}$$

the vibrational, or Franck–Condon overlap $\langle\phi_b|\phi_a\rangle$ contained in the transition matrix elements T_{ba}, is not restricted to separable vibration states; ϕ_a, ϕ_b are the vibration state functions of the initial and final state in diabatic or quasi-adiabatic potentials. In Eq. (1), ΔE^{vib} is the change of vibration energy in the conversion process, ΔE the difference of total energy zero points of states (a) and (b), Av indicates thermal weighting. Taking into consideration general potential surface characteristics, the question of including non-separable anharmonic vibrations in the transition matrix treatment arises.

Calculation of vibration states in non-separable systems has received much attention over the last decade [3–6]. Semiclassical quantization, as well as variational approximations using expansions in terms of products of harmonic functions reveal, in general, stable (or regular) vibrations in lower quantum states.

Pursuing the question raised above, we have applied a numerical random walk sampling technique for the *ab initio* solution of the Schrödinger equation. This method was devised recently for the calculation of many-electron total energies including electron correlation [7, 8], but it is also suited to vibration problems [9]. The method works as follows: in imaginary time $t = t_{\text{real}} \cdot i/\hbar$, the Schrödinger equation assumes the form of a diffusion equation

$$\partial\phi/\partial t = D\,\nabla^2\phi - V\phi, \qquad D = \hbar^2/2\mu. \tag{2}$$

Using a known trial wave function ϕ_T, one gets a diffusion equation with a reaction and a drift term for the product function $f(t) = \phi(t) \cdot \phi_T$:

$$\partial f/\partial t = D\,\nabla^2 f - (E_L - E_{\text{ref}})f - D\,\nabla f F, \tag{3}$$

where $E_L = H\phi_T/\phi_T$ is a local energy, E_{ref} a reference energy, and $F = \nabla \ln|\phi_T|^2$ a quantum drift velocity. The propagator for Eq. (3) is the Green's function [8, 10]

$$G(R, R', \Delta t) = (4\pi D\,\Delta t)^{-N/2} \exp\left\{-\frac{[R' - R - D\,\Delta t \cdot F(R)]^2}{4D\,\Delta t}\right\} \times \exp\{-[(E_L(R) + E_L(R'))/2 - E_{\text{ref}}]\,\Delta t\}, \tag{4}$$

from which

$$f(R', t + \Delta t) = \int dR G(R, R', \Delta t) f(R, t) \tag{5}$$

is sampled. The total energy is obtained from $\langle E_L \rangle$. N in (4) is the dimension of the vector space R. Propagation using Eqs. (4, 5) yields the stationary ground state; excited states are accessible, from, e.g., orthogonalization or fixed node constraints [7–9].

2. An example of vibration in anharmonic 2D potential surfaces

As well as the total energy, we are particularly interested in the wave function $\phi = f/\phi_T$ which can be sampled together with energy. We begin with considering the vibration ground state in a two-dimensional (2D) potential surface in cartesian coordinates.

As a trial function ϕ_T in Eqs. (3, 4) one may use the known solution of the Schrödinger equation with the separable hamiltonian:

$$\nabla^2 = \partial^2/\partial x^2 + \partial^2/\partial y^2; \qquad V = V_1(x) + V_2(y). \tag{6}$$

As an example we consider a superposition of a Morse and a harmonic potential component:

$$V_1(x) = D_1[1 - \exp(-ax)]^2; \qquad V_2(y) = (k_2/2)y^2. \tag{7}$$

$D_1 = k_1/2a^2$ is a bond dissociation energy, a is the anharmonicity constant, k are harmonic force constants. The x-coordinate may represent the reaction path of a diabatic Franck–Condon model. Separability of the vibrations in the potential (6, 7) holds when D_1 and a are independent of y, and k_2 is independent of x.

If one removes this constraint, e.g. by taking an x-dependent force constant $k_2(x)$, one gets an additional non-separable potential component V_3:

$$V = V_1(x) + V_2(y) + V_3(x, y), \tag{8}$$

where V_2 is given by (7) taken at $x = 0$. Let us assume the following simple form for k_2:

$$k_2 = k_2(0)(1 - bx). \tag{9}$$

One then obtains

$$V_3(x, y) = -\frac{k_2(0)b}{2} xy^2, \tag{10}$$

which resembles a Henon–Heiles potential (cf. also [3–6]). The valleys at $bx > 1$ are not attained in the following sampling experiments.

3. Calculations

Quantum random walk sampling following Eqs. (3–5) may be illustrated on a system obeying Eqs. (6–10) with the following scaled parameter values:

$$k_1 = k_2(0) = 1; \qquad D_1 = 12.5; \qquad a = 0.2; \qquad \hbar\omega = 1; \qquad b = 0.05. \tag{11}$$

If we take energy and length units 0.2 eV and 10 pm, respectively, these parameters become $k_1 = k_2(0) = 2000\ \text{eV nm}^{-2} = 320\ \text{kg s}^{-1}$; $D_1 = 2.5$ eV; $a = 20\ \text{nm}^{-1}$; $\hbar\omega = 0.2$ eV, corresponding to a reduced mass $\simeq 2$; $b = 5\ \text{nm}^{-1}$. With (11) the ground state function of a harmonic 1D mode is

$$\phi^{1D}_{harm} = 0.7511 \exp(-x^2/2), \tag{12}$$

and that of a Morse 1D mode

$$\phi^{1D}_{Morse} = \left[\frac{a}{(\alpha - 1)!}\right]^{1/2} \exp(-z/2) z^{\alpha/2}, \tag{13}$$

where $\alpha = 2k_1/a^2\hbar\omega - 1 = 49$ and $z = 50 \exp(-0.2x)$. The corresponding energy eigenvalues are $E^{1D}_{harm} = 0.5$ and $E^{1D}_{Morse} = 0.495$.

Sampling the energy of the 1D Morse oscillator with the harmonic Eq. (12) as trial function, gave, for 500 configurations, a time step width $\Delta t = 0.01$, and 27300 steps in 13 sections (for calculating the variance):

$$E^{1D}_{Morse}(\text{sampled}) = 0.49544 \pm 0.00036.$$

Results for the 1D Morse wave function are shown in Fig. 1. Again using Eq. (12) as trial function, the sampled function $(f/\phi_T - \phi_T)$ is compared with the exact difference $(\phi^{1D}_{Morse} - \phi^{1D}_{harm})$. When a smaller time step, $\Delta t = 0.0033$, was used the agreement on the positive branch $x > 0$, where the harmonic trial

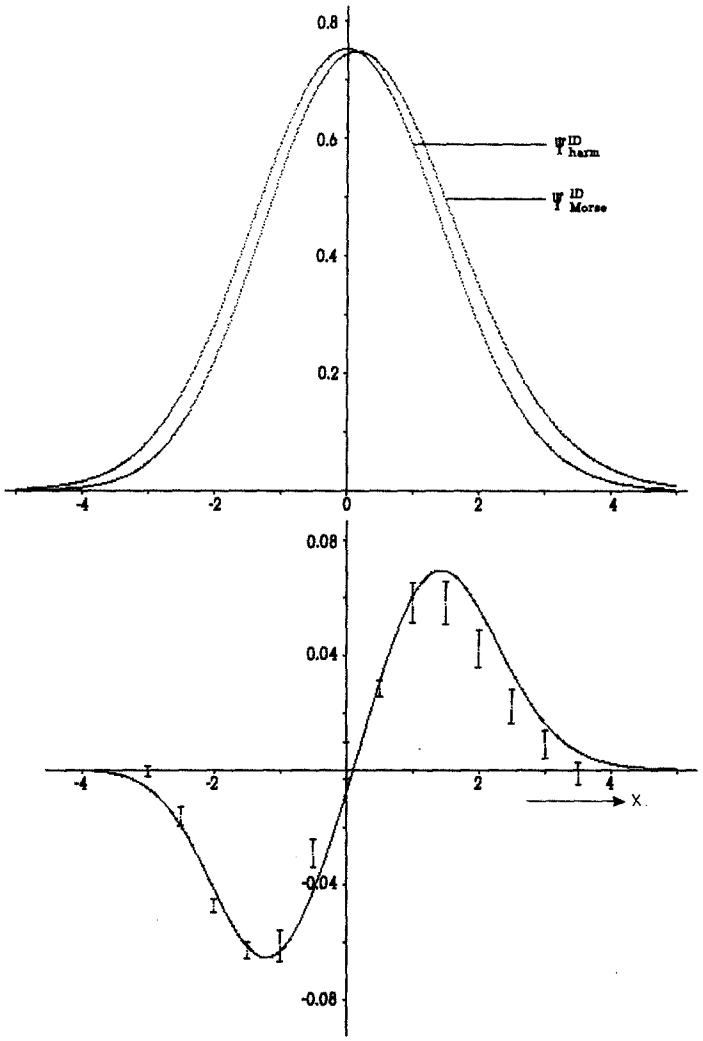

Fig. 1. 1D harmonic and Morse ground-state function (*top*). Analytically calculated difference function ($\phi^{1D}_{Morse} - \phi^{1D}_{harm}$) from Eqs. (12, 13) (*bottom, solid line*) compared with sampled difference function ($f/\phi_T - \phi_T$) with $\phi_T = \phi^{1D}_{harm}$. For parameter values and discussion see text. 30000 time steps in 10 sections, time step width $\Delta t = 0.0033$ are used

function deviates increasingly from the Morse function, was slightly better. A typical time-step dependence of sampled wave function values is illustrated in Fig. 2. These data support the reliability of the method.

3.1. 2D vibration state

Simulation of the 2D vibration problem following Eqs. (6–10) has been carried through with the product $\phi^{1D}_{Morse}(x)\phi^{1D}_{harm}(y)$ as a trial function. This corresponds

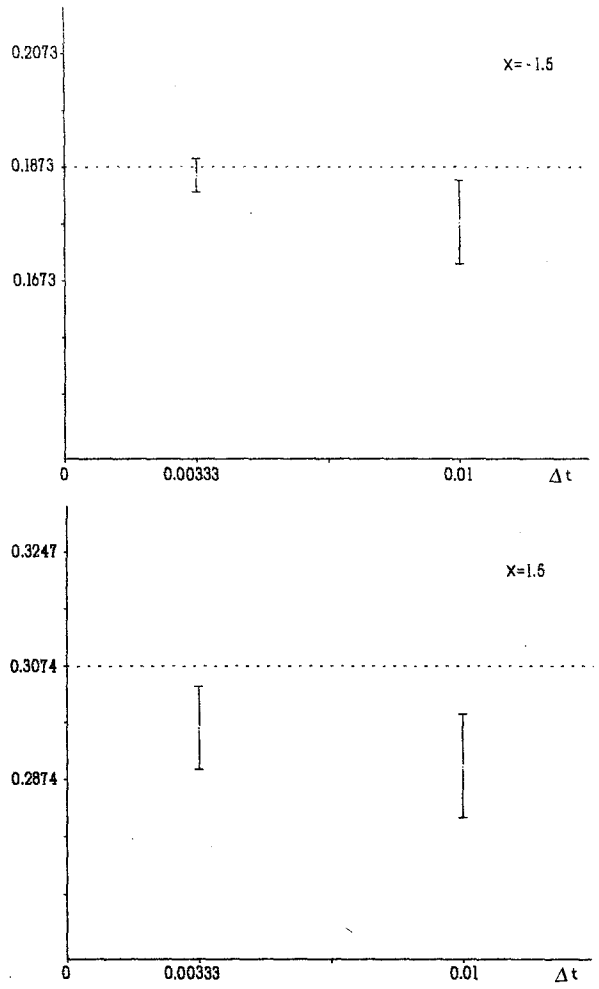

Fig. 2. Time step dependence of the sampled 1D Morse function $\phi = f/\phi_T$ at $x = -1.5$ (*top*) and $+1.5$ (*bottom*). The *dotted line* marks the exact Morse function values

to the neglect of V_3 in Eq. (8). The corresponding ground state energy is 0.995. Sampling the full hamiltonian including V_3 gave (with 500 configurations in 20 runs of 2000 time steps of length $\Delta t = 0.01$):

$$E^{2D} = 0.992996 \pm 0.000036.$$

Figure 3 illustrates the evolution of the mean value E^{2D} and of the standard deviation from the 20 runs. The sampled mean value has lost its memory of the (arbitrary) initial distribution of configurations after some 10^2 time steps.

The 2D difference function $(\phi^{2D} - \phi_T^{2D})$ was sampled in boxes 0.04×0.04. Figure 4 shows cross-sections of the 2D difference function parallel to the x-axis which, despite the relatively large variance, yield significant information about the order of magnitude of the effect of the non-separable potential component V_3

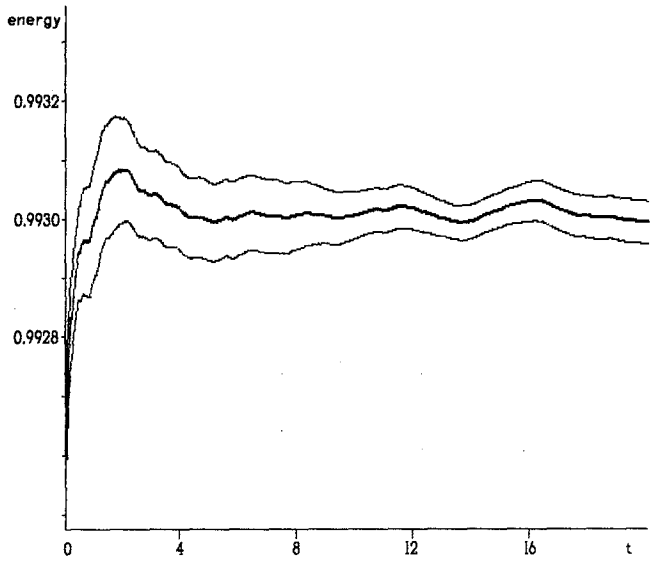

Fig. 3. Evolution of the mean value, E^{2D}, and the standard deviation from 20 runs of 2000 time steps of length $\Delta t = 0.01$

upon the wave function. For comparison, the value of the wave function at (0, 0), i.e. near its maximum, is $\phi(0, 0) \approx 0.55$.

3.2. Franck–Condon overlap

The overlap of the vibration functions ϕ_a, ϕ_b on two potential surfaces can be expressed in terms of the corresponding trial functions and first-order corrections:

$$\langle \phi_b | \phi_a \rangle \simeq \langle \phi_{Tb} | \phi_{Ta} \rangle + \langle \phi_{Tb} | \alpha \rangle + \langle \beta | \phi_{Ta} \rangle, \tag{14}$$

where

$$\alpha = \phi_a - \phi_{Ta}, \qquad \beta = \phi_b - \phi_{Tb}, \tag{15}$$

are assumed to be small (for the possible breakdown of this assumption see below).

Equation (14) has been evaluated for two opposed potentials of equal form, following Sect. 3.1, but the opposed one with an anharmonicity constant $a = -0.2$ and displaced along the x-coordinate by Δx. The following statements can be made.

(a) The overlap of the trial functions $\langle \phi_{Tb} | \phi_{Ta} \rangle$ (the first term of Eq. (14)) can be calculated without noticeable error by numerical integration.

(b) The first-order correction terms in (14) equal $2\langle \phi_{Tb} | \alpha \rangle$, because the same potential forms are assumed for both cases. Calculation of this 2D integral has been performed on a grid.

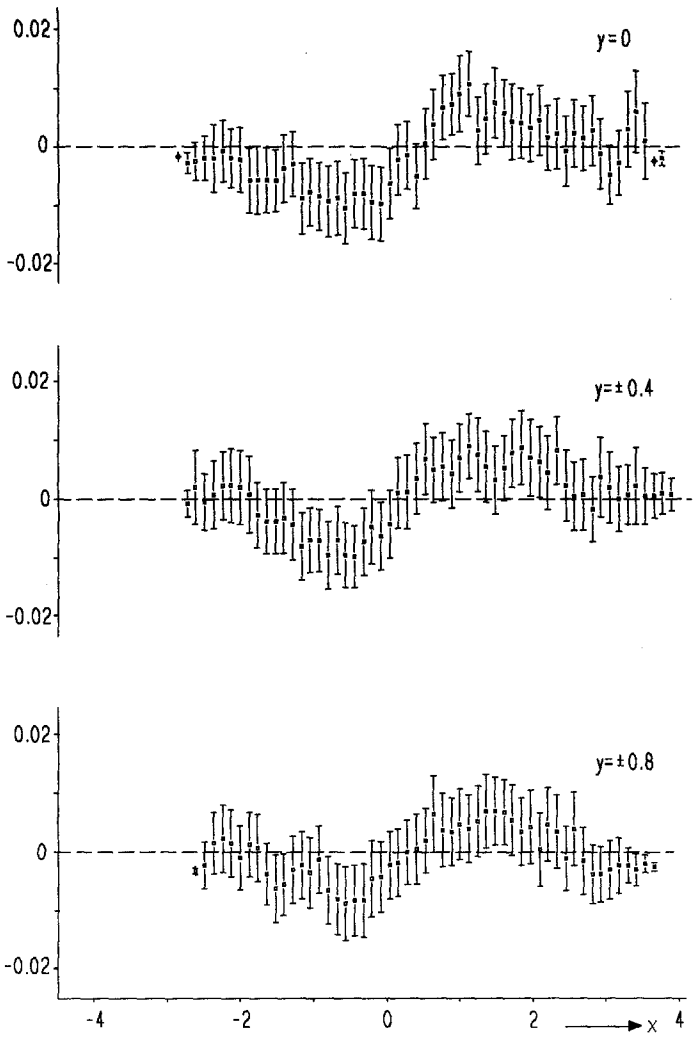

Fig. 4. Cross-sections of the 2D difference function ($\phi^{2D} - \phi_T^{2D}$) parallel to the x-axis, at $y = 0$, ± 0.4 and ± 0.8 (preliminary data). For $|y| \gtrsim 2$ the mean value of the difference function falls below the error limit. 20 runs of 1000 time steps of length $\Delta t = 0.01$ are used. Sampling is in boxes 0.04×0.04; the results are smooth by averaging over nearest-neighbour boxes. Improvement of data is possible at greater expense

(c) Due to increase of $|V_3|$ with increasing x, the relative deviation of the tail of the exact wave function ϕ_b from ϕ_{Tb} increases. This tail enters with increasing weight into the overlap integral when the distance Δx becomes large. Because of increasing relative error in the tails of the difference function α, the overlap $\langle \phi_{Tb} | \alpha \rangle$ becomes less accurate at larger displacement of the both potential minima.

(d) Thus, at large Δx, the tails of $\alpha(x, y)$ and $\beta = \alpha(\Delta x - x, y)$ dominate the total Franck–Condon overlap, and the first-order correction $2\langle \phi_{Tb} | \alpha \rangle$ can be

Table 1. Franck–Condon overlap of the 2D trial functions and preliminary data for the first-order correction as a function of the spatial displacement Δx (see text)

Δx[a]	0	2	4	5	6
$\langle \phi_{Tb} \vert \phi_{Ta} \rangle$	0.976	0.52	5.3×10^{-2}	10.0×10^{-3}	14.1×10^{-4}
$2\langle \phi_{Tb} \vert \alpha \rangle$[b]	-0.01 ± 0.006[c]	0.02 ± 0.01	$(0.4 \pm 0.2) \times 10^{-2}$	$(3 \pm 1) \times 10^{-3}$	$(7.5 \pm 3) \times 10^{-4}$

[a] Unit of length 10 pm

[b] Mean value and variance of the Franck–Condon integral is calculated from mean values of $\alpha(x, y)$ from independent runs. The sampled difference function $\alpha(x, y)$ was set to zero in boxes with no configurations

[c] The negative sign at $\Delta x = 0$ is due to the greater weight of ϕ_{Tb} at $x < 0$

large or even larger than the trial function overlap $\langle \phi_{Tb} \vert \phi_{Ta} \rangle$. The integral $\langle \beta \vert \alpha \rangle$ must then be added to (14). Alternatively $\langle \phi_b \vert \phi_a \rangle$ may be calculated without decomposition.

Some Frank–Condon overlaps of separable trial functions and of first-order corrections due to the non-separable potential component V_3 are given in Table 1 for different spatial displacements Δx of the 2D potential surfaces. The increase in the relative correction $2\langle \phi_{Tb} \vert \alpha \rangle / \langle \phi_{Tb} \vert \phi_{Ta} \rangle$ with increasing Δx is apparent. Great care must be taken with the extrapolation of these preliminary data up to larger reactive transfer distances [11]. The present data suggest the possibility of significant corrections to Frank–Condon overlap due to the non-separable potential component, even in ground-state transitions.

4. Discussion

Simulation of many-dimensional wave functions and derived quantities is significantly more expensive than that of total energy. Several questions of a general nature can however be studied on this line, already on two-dimensional model cases.

The results of Sect. 3 provide a first clue to the effect of non-separable potential components upon vibration energies, wave functions and Franck–Condon overlaps of vibration ground states, being relevant for large vibration quanta and low temperature. Larger non-separability effects are expected for excited vibration states; extension of the present simulation technique to such cases is straightforward but more expensive (as is the case for any quantum simulation). The present orientational calculations were made on 16-bit computers and can be further refined.

From a theoretical point of view, the following points may briefly be addressed:

(i) In principle, by means of the applied quantum simulation, we obtain exact eigenstates of the Schrödinger equation for non-separable (multidimensional) vibrations, within known error limits. We can presume that these eigenstates are

relevant for Franck–Condon transitions except those with lifetimes of the initial states $<10^{-9}$ to 10^{-12} s. (For these conditions incomplete relaxation after preceding reactive or dephasing processes, as well as interference from bimolecular encounter comes into play.)

(ii) The approach of the real-time evolution of vibrational wave packets in non-separable potentials (cf., e.g., [12]) is in certain respect complementary to the present one. A more detailed comparison requires knowledge of higher quantum states.

(iii) Non-separable systems of the type under discussion may have either semiclassical regularity or irregularity [4, 5]. Quantum behaviour under the condition of semiclassical irregularity may be proved by following the present approach.

The extension of this study to low excited states is in progress.

References

1. Lorenz W (1979) Z phys Chem 260:241; (1987) phys stat sol B144:585
2. Lorenz W, Engler C (1984) phys stat sol B122:745
3. Chapman S, Garrett BC, Miller WH (1976) J Chem Phys 64:502
4. Swimm RT, Delos JB (1979) J Chem Phys 71:1706; Shirts RB, Reinhardt WP (1982) J Chem Phys 77:5204
5. Martens CC, Ezra GS (1987) J Chem Phys 86:279
6. Christoffel KM, Bowman JM (1981) J Chem Phys 74:5057
7. Anderson JB (1975) J Chem Phys 63:1499; (1976) J Chem Phys 65:4121; (1985) J Chem Phys 82:2662
8. Reynolds PJ, Ceperley DM, Alder BJ, Lester WA (1982) J Chem Phys 77:5593; Ceperley DM, Alder BJ (1984) J Chem Phys 81:5833
9. Cocker DF, Watts RO (1986) Mol Phys 58:1113
10. Kalos MH (1962) Phys Rev 128:1791
11. Engler C, Rabe E, Schultz H, Lorenz W (1989) Theor Chim Acta 75:67
12. Park TJ, Light JC (1986) J Chem Phys 85:5870